ISSN 1063-7761, Journal of Experimental and Theoretical Physics, 2019, Vol. 128, No. 6, pp. 885–898. © Pleiades Publishing, Inc., 2019.
Russian Text © The Author(s), 2019, published in Zhurnal Eksperimental'noi i Teoreticheskoi Fiziki, 2019, Vol. 155, No. 6, pp. 1045–1060.

ORDER, DISORDER, AND PHASE TRANSITION IN CONDENSED SYSTEM

Strong Spin–Charge Coupling and Its Manifestation in the Quasiparticle Structure, Cooper Instability, and Electromagnetic Properties of Cuprates

V. V. Val'kov[a,*], D. M. Dzembisashvili[a,b], M. M. Korovushkin[a], K. K. Komarov[a], and A. F. Barabanov[c]

[a] *Kirensky Institute of Physics, Federal Research Center "Krasnoyarsk Scientific Center," Siberian Branch, Russian Academy of Sciences, Krasnoyarsk, 660036 Russia*

[b] *Reshetnikov Siberian State University of Science and Technology, Krasnoyarsk, 660037 Russia*

[c] *Vereshchagin Institute of High-Pressure Physics, Russian Academy of Sciences, Troitsk, Moscow, 108840 Russia*

**e-mail: vvv@iph.krasn.ru*

Received November 20, 2018; revised November 20, 2018; accepted December 18, 2018

Abstract—The Fermi excitation spectrum, the problem of Cooper instability, and the Londons magnetic field penetration depth in cuprate superconductors are considered using the unified conception based on accounting for the strong coupling between the spin of copper ions and holes at oxygen ions. This coupling leads to strong renormalization of the primary spectrum of oxygen holes with the formation of spin-polaron quasiparticles. Analysis of Cooper instability performed using the spin-polaron concept for different channels has shown that only the superconducting *d*-wave pairing occurs in the ensemble of spin-polaron quasiparticles, and there are no solutions corresponding to the *s*-wave pairing. It has been demonstrated that the superconducting *d*-wave pairing is not suppressed by the Coulomb repulsion of holes located at neighboring oxygen ions. This effect is due to peculiarities in the crystallographic structure of the CuO_2 plane and the aforementioned strong spin–fermion coupling. As a result, such interaction of holes is omitted in the kernel of the integral equation for the superconducting order parameter with the *d*-wave symmetry. It has been shown the Hubbard repulsion of holes and their interaction for the second coordination sphere of the oxygen sublattice for actual intensities of the interaction do not suppress the *d*-wave type of superconductivity. For the spin-polaron ensemble, we have analyzed the dependence of the Londons magnetic field penetration depth on the temperature and hole concentration. It has been established that the peculiarities of this dependence are closely related to specific features of the spin-polaron spectrum.

DOI: 10.1134/S1063776119050078

1. INTRODUCTION

It is well known that the central problem in the theory of high-temperature superconductivity is the necessity of correct accounting for strong electron correlations that not only change qualitatively the ground state of these materials in the normal phase, but also lead to a new scenario of Cooper instability.

The electronic structure of cuprates is correctly described by the Emery model [1, 2] or by its more general variant [3] in which peculiarities of the crystallographic structure of the CuO_2 plane are considered as well as the hole states in closed shells of copper and oxygen ions. The energy parameters of the Emery model correspond to the regime of strong electron correlations and make it possible to integrate the contributions from covalent mixing between the *d*- and *p*-states of copper and oxygen ions by passing to the effective Hamiltonian. Such a procedure can be performed most easily on the basis of the operator form of perturbation theory in the atomic representation using the Hubbard operators [4]. As a result, the spin–fermion model (SFM) is constructed [5–10] with Hamiltonian H_{sp-f}, in which the space of states of copper ions is limited to the class of homeopolar states. For the undoped regime, the SFM degenerates into the Heisenberg model with antiferromagnetic (AFM) type of the exchange interaction between the nearest spins of copper ions.

It is known that in the theory of cuprate superconductors, the strong coupling between the spin and charge degrees of freedom plays an important role [11–14]. Spin–charge fluctuations considerably affect the thermodynamic and transport properties of cuprate superconductors [15]. The SFM contains terms reflecting spin–charge fluctuations between localized spins of copper ions and oxygen holes. In particular, such terms correspond to spin-correlated jumps [16–18] as a result of which charge transfer with

simultaneous change of the spin projection at an oxygen hole occurs. In accordance with the law of conservation of the total spin projection of the entire system, the spin projection at a copper ion changes. Significantly, the spin–fermion coupling parameters are large and cannot be considered in conventional perturbation theory. This considerably complicates the problem of inclusion of the strong spin–charge coupling in cuprate superconductors.

It should be emphasized that in contrast to simplified models of the electronic structure of cuprates (such as the Hubbard model or the t–J model), the SFM contains the description of the actual structure of the CuO_2 plane, in which the unit cell includes two oxygen ions and one copper ion. In addition, the spatial separation of the spin and charge subsystems is also considered in the SFM.

In the SFM, the spin-polaron conception has been developed [16, 17, 19–21], which has made it possible to correctly describe peculiarities in the spectral properties of Fermi quasiparticles of cuprate semiconductors in the normal phase. The original idea of this conception is that an elementary excitation in a doped 2D antiferromagnet can be represented as a "bare" particle (electron or hole) surrounded by a cloud of spin fluctuations [21]. This composite quasiparticle, which has a renormalized mass and moves against the background of AFM ordering, is treated as a spin polaron. The simplest example of such a quasiparticle is a local spin polaron [22, 23], the characteristics of which are determined from the solution of the cluster problem. Having chosen the lowermost energy states of a small cluster, it is possible to describe the motion of a local spin polaron against the background of AFM ordering.

Using the concept of the spin polaron in the SFM, the splitting of the lower band of a local polaron was investigated [24], which made it possible, for example, to describe the sharp decrease in the ARPES peak intensities upon a change in the quasi-momentum from $(\pi/2, \pi/2)$ to (π, π) or $(0, 0)$ as well as the possibility of existence of a "shadow zone" [25].

It was shown in [16, 26] that, in contrast to the tight binding models with a large number of fitting parameters (see, for example, [27]), the modification of the energy spectrum and the Fermi surface in the SFM with the spin-polaron conception is associated not with the relation between hopping integrals, but with a strong correlation between the subsystem of localized spins of copper ions in the state of the quantum spin liquid and the subsystem of oxygen holes, as well as with a change in the correlation characteristics of this quantum spin liquid upon doping. In [26], only one fitting parameter (hole hopping integral t) was used, which was selected from comparison with experimental data [27] for $La_{2-x}Sr_xCuO_4$. It should be noted that the authors of [27] had to select a set of four parameters (three hopping integrals t_1, t_2, t_3, and energy shift ε_0) for attaining a satisfactory agreement between the Fermi surface calculated in the mean field approximation and the Fermi surface reconstructed from experimental data for each hole concentration level.

The successful description of the properties of cuprates in the normal state using the spin polaron concept suggested the possibility of describing the superconducting phase in the conditions when the Cooper instability evolves not for seeding fermions, but in the subsystem of spin polarons [28]. It was shown in [29] that an ensemble of spin-polaron quasiparticles appearing in the simplest model of cuprate superconductors (2D Kondo lattice) in the regime of strong electron correlations exhibits Cooper instability with $d_{x^2-y^2}$-wave type of the order parameter symmetry. As the Cooper pairing constant, the integral of exchange interaction between localized spins was used. It was shown that in contrast to the t–J^* model [30], three-centered interactions in the spin-polaron ensemble in the spin-liquid phase of the localized spin subsystem facilitate Cooper pairing and ensure the realization of the superconducting phase with high superconducting transition temperatures.

Later, the theory of superconductivity of a spin polaron ensemble was developed in the SFM in [31]. It was shown that the strong spin–fermion coupling emerging as a result of hybridization mixing of the states of copper and oxygen ions in the original Emery model not only affects the formation of spin-polaron quasiparticles [20], but also ensures effective attraction between them. This induces Cooper instability with the d-wave pairing in the spin polaron system. This approach was used for constructing the T–x phase diagram [31] which correlated well with experimental data on cuprate superconductors.

An important result obtained for further development of the spin-polaron conception [31] was the solution of the problem that appeared soon after the first theoretical publications on superconductivity in HTSCs. This problem was associated with the fact that intersite Coulomb interaction V_1 between holes at the nearest oxygen ions, which was considered using effective low-energy models on a square lattice, led to suppression of superconducting pairing with the d-wave type of the order parameter symmetry. It was shown in [32] that neutralization of the negative effect of intersite Coulomb interaction of holes on Cooper instability in the d-wave channel occurs due to the operation of the following two factors. The first factor is associated with analysis of the actual crystallographic structure of the CuO_2 plane, for which the Fourier transform of the inter-site interaction has the form

$$V_q = 4V_1 \cos(q_x/2)\cos(q_y/2).$$

The second factor is due to the strong coupling between localized spins of copper ions and holes at oxygen ions. As shown in [31], this leads to the evolu-

tion of Cooper instability in an ensemble of spin-polaron quasiparticles. In this case, the Coulomb repulsion between bare holes with Fourier transform V_q is renormalized into the interaction between spin-polaron quasiparticles so that the momentum dependence of this effective interaction corresponds to the relevant structure of the copper ion sublattice. As a result, the situation appears, in which the effective repulsion between spin polarons is omitted from the kernel of the integral equation for the superconducting order parameter with the $d_{x^2-y^2}$-wave symmetry type.

The effect of Coulomb repulsion V_2 of holes located at the second-neighbor oxygen ions was considered later in [33, 34], and the effect of Hubbard repulsion U_p of holes on the concentration dependences of the superconducting transition temperature was analyzed in [35]. It was shown that the inclusion of the above interactions gives lower values of the superconducting transition temperature; however, this temperature remains within the range of experimentally observed values.

The possibility of emergence of superconducting *s*-wave pairing of spin-polaron quasiparticles was analyzed in [35] using the SFM. The calculated dependence of the superconducting transition temperature on the doping level revealed that the solutions of self-consistent equations in the entire range of doping levels correspond to only the $d_{x^2-y^2}$-wave phase, while the solutions for the *s*-wave phase are absent. This result is in complete agreement with experimental data on cuprate superconductors.

Due to the aforementioned successful application of the spin polaron conception for describing the electronic structure and superconducting properties of cuprate superconductors, the complex of problems associated with the study of kinetic and galvanomagnetic properties of these materials has become topical. In particular, the calculation of the Londons magnetic field penetration depth in a cuprate superconductor in which charge carriers are not seed fermions [36–40], but spin-polaron quasiparticles formed due to strong coupling between the spin and charge degrees of freedom is of considerable interest. In this study, we report on the most important results on the theory of cuprate superconductors, which were obtained using the spin-polaron concept in the SFM.

The article is organized as follows. In Section 2, we describe the SFM following from the three-band *p–d* model in the regime of strong electron correlations. Section 3 is devoted to derivation of equations for the normal and anomalous Green functions. The system of integral equations for the superconducting order parameter component is also considered. In Section 4, we analyze the energy structure of spin-polaron quasiparticles. The superconducting phase of spin polarons is considered in Section 5. In particular, we consider the effect of the intersite Coulomb interaction on the evolution of Cooper instability of an ensemble of spin polarons and demonstrate the stability of the superconducting *d*-wave pairing to the inclusion of the Coulomb repulsion of holes located at neighboring oxygen ions. On the basis of calculated concentration dependences of the superconducting transition temperature, we analyze the effect of the Hubbard interaction and Coulomb repulsion of holes located at the next-to-neighboring oxygen ions. In Section 6, the Londons magnetic field penetration depth in a cuprate superconductor, in which spin-polaron quasiparticles play the role of charge carriers, is calculated. The results are discussed in concluding Section 7. For convenience of presentation, cumbersome analytic expressions are given in Appendix.

2. SPIN–FERMION MODEL

According to experimental data, in the undoped case with a single hole per unit cell on the CuO_2 plane, the system is in the state of the Mott–Hubbard insulator [41]. In the three-band *p–d* (Emery) model [1, 2], this case corresponds to the regime of strong electron correlations,

$$\Delta_{pq}, (U_d - \Delta_{pd}) \gg t_{pd} > 0. \quad (1)$$

On the one hand, these inequalities require correct accounting for Coulomb correlations at a copper ion, while on the other hand, these inequalities make it possible to perform reduction of the Hamiltonian in the Emery model and obtain the SFM [5–10] with Hamiltonian

$$\hat{H}_{sp-f} = \hat{H}_h + \hat{U}_p + \hat{V}_{pp} + \hat{J} + \hat{I}, \quad (2)$$

where

$$\hat{H}_h = \sum_{k\alpha} (\xi_{k_x} a^\dagger_{k\alpha} a_{k\alpha} + \xi_{k_y} b^\dagger_{k\alpha} b_{k\alpha} + t_k (a^\dagger_{k\alpha} b_{k\alpha} + b^\dagger_{k\alpha} a_{k\alpha})), \quad (3)$$

$$\hat{U}_p = \frac{U_p}{N} \sum_{1,2,3,4} [a^\dagger_{1\uparrow} a^\dagger_{2\downarrow} a_{3\downarrow} a_{4\uparrow} + (a \to b)] \delta_{1+2-3-4}, \quad (4)$$

$$\hat{V}_{pp} = \frac{4V_1}{N} \sum_{\substack{1,2,3,4 \\ \alpha,\beta}} \phi_{3-2} a^\dagger_{1\alpha} b^\dagger_{2\beta} b_{3\beta} a_{4\alpha} \delta_{1+2-3-4}$$
$$+ \frac{V_2}{N} \sum_{\substack{1,2,3,4 \\ \alpha,\beta}} [\theta^{xy}_{2-3} a^\dagger_{1\alpha} a^\dagger_{2\beta} a_{3\beta} a_{4\alpha} + \theta^{yx}_{2-3} (a \to b)] \delta_{1+2-3-4}, \quad (5)$$

$$\hat{J} = \frac{J}{N} \sum_{fkq\alpha\beta} e^{if(q-k)} u^\dagger_{k\alpha} (\mathbf{S}_f \cdot \boldsymbol{\sigma}_{\alpha\beta}) u_{q\beta}, \quad (6)$$

$$\hat{I} = \frac{I}{2} \sum_{f\delta} \mathbf{S}_f \cdot \mathbf{S}_{f+2\delta}. \quad (7)$$

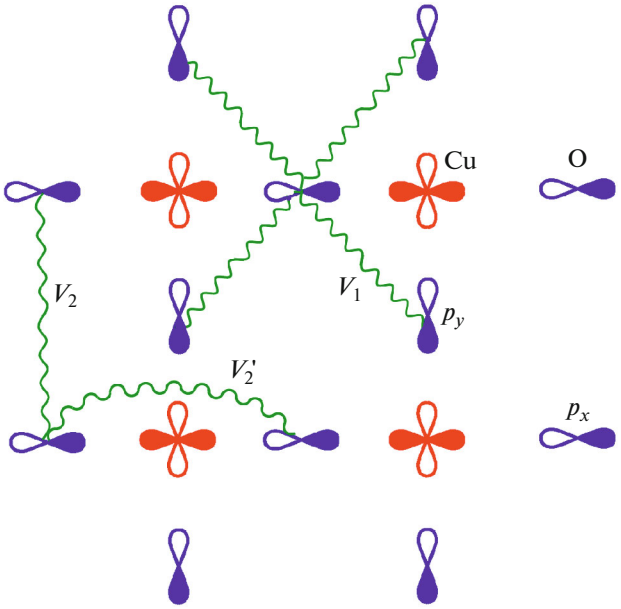

Fig. 1. (Color online) Structure of the CuO_2 plane. V_1 denotes the Coulomb interaction of holes locates at the nearest oxygen ions, V_2 and V_2' are the Coulomb repulsions of holes located at the next-to-nearest oxygen ions.

Here, we have introduced the following notation:

$$\xi_{k_{x(y)}} = \tilde{\varepsilon}_p + \tau(1 - \cos k_{x(y)}) - \mu,$$
$$\tilde{\varepsilon}_p = \varepsilon_p + 2V_{pd}, \quad t_k = (2\tau - 4t)s_{k,x}s_{k,y},$$
$$\theta_k^{xy(yx)} = \frac{V_2'}{V_2}\exp(ik_{x(y)}) + \exp(-ik_{y(x)}),$$
$$s_{k,x} = \sin\frac{k_x}{2}, \quad u_{k\beta} = s_{k,x}a_{k\beta} + s_{k,y}b_{k\beta}, \qquad (8)$$
$$\tau = \frac{t_{pd}^2}{\Delta_{pd}}\left(1 - \frac{\Delta_{pd}}{U_d - \Delta_{pd} - 2V_{pd}}\right),$$
$$J = \frac{4t_{pd}^2}{\Delta_{pd}}\left(1 + \frac{\Delta_{pd}}{U_d - \Delta_{pd} - 2V_{pd}}\right).$$

Operator $\hat{H}_h$ (3) described the subsystem of holes at oxygen ions in the quasi-momentum representation. Here, $a_{k\alpha}^{\dagger}(a_{k\alpha})$ are the creation (annihilation) operators for holes in the oxygen subsystem with p_x orbitals (Fig. 1) and $\alpha = \pm 1/2$ is the spin projection. Analogously, operators $b_{k\alpha}^{\dagger}(b_{k\alpha})$ describe the subsystem of oxygen ions with the p_y orbitals. The one-site hole energy is denoted by ε_p, μ is the chemical potential of the system, and t is the hopping integral.

Operator $\hat{U}_p$ (4) describes the Hubbard repulsion of holes at oxygen ions. The intersite Coulomb interactions of holes located at second-neighbor oxygen ions (see Fig. 1) are described by operator $\hat{V}_{pp}$ (5). Operator $\hat{J}$ (6) corresponds to the exchange interaction between the oxygen hole subsystem and the subsystem of spins localized at copper ions, which are described by operators $\mathbf{S}_f$. Here, $\boldsymbol{\sigma} = (\sigma^x, \sigma^y, \sigma^z)$ is the vector composed of Pauli matrices. Operators $\hat{I}$ (7) describes the superexchange interaction between the nearest-neighbor spins of copper, which appears in the fourth order of perturbation theory.

In the expression for SFM Hamiltonian, the signs of the hopping integrals depending on the direction of jump and the phase of wavefunctions are considered. For compactness, the quasi-momenta over which summation is performed are denoted by numbers 1, ..., 4. Dirac delta function $\delta_{1+2-3-4}$ takes into account the momentum conservation law.

In the further calculation of the energy structure and in analysis of the conditions for evolution of Cooper instability in the SFM, we will use the generally accepted notation for the parameters in the Emery model [42, 43]: $t_{pd} = 1.3$, $\Delta_{pd} = 3.6$, and $V_{pd} = 1.2$ (in electronvolts). For the hopping integral of holes between oxygen ions, notation $t = 0.12$ eV is used [26], and the constant of exchange interaction between spins at copper ions is chosen as $I = 0.136$ eV, which agrees with the available experimental data on cuprate superconductors. The parameters of Coulomb repulsion of holes at the nearest and next-to-nearest oxygen ions are chosen to be $V_1 = 1$–2 eV [44] and $V_2 = V_2' = 0.5$–1.0 eV, respectively.

3. SYSTEM OF EQUATIONS FOR GREEN'S FUNCTIONS

Since the intensity of the exchange interaction between localized spins of copper and spins of holes at oxygen ions is found to be high ($J = 3.38$ eV $\gg \tau \approx 0.10$ eV), this coupling should be accounted for rigorously in calculation of the energy structure of spin-polaron excitations and in analysis of conditions for the emergence of superconducting pairing. For this purpose, it is convenient to use the Zwanzig–Mori projection method [45–47]; the application of this method with the SFM is described in detail in [20, 26, 31].

To take into account the aforementioned spin–charge coupling correctly, it is fundamentally important to introduce into the basis set (apart from operators $a_{k\alpha}$ and $b_{k\alpha}$) the operator

$$L_{k\alpha} = \frac{1}{N}\sum_{fq\beta} e^{if(q-k)}(\mathbf{S}_f \cdot \boldsymbol{\sigma}_{\alpha\beta})u_{q\beta}. \qquad (9)$$

For analyzing the conditions for the emergence of Cooper instability, the above set of three operators should be supplemented with three more operators [31, 32] ($\bar{\alpha} = -\alpha$)

$$a^{\dagger}_{-k\bar{\alpha}}, \quad b^{\dagger}_{-k\bar{\alpha}}, \quad L^{\dagger}_{-k\bar{\alpha}}, \tag{10}$$

which make it possible to introduce anomalous thermodynamic means.

The complete system of equations for normal G_{ij} and anomalous F_{ij} Green's function ($j = 1, 2, 3$), which was obtained using the projection method, has the form

$$\begin{aligned}
(\omega - \xi_x)G_{1j} &= \delta_{1j} + t_k G_{2j} + J_x G_{3j} + \Delta_{1k}F_{1j} + \Delta_{2k}F_{2j},\\
(\omega - \xi_y)G_{2j} &= \delta_{2j} + t_k G_{1j} + J_y G_{3j} + \Delta_{3k}F_{1j} + \Delta_{4k}F_{1j},\\
(\omega - \xi_L)G_{3j} &= \delta_{3j}K_k + (J_x G_{1j} + J_y G_{2j})K_k + \frac{\Delta_{5k}}{K_k}F_{3j},\\
(\omega + \xi_x)F_{1j} &= \Delta^{*}_{1k}G_{1j} + \Delta^{*}_{3k}G_{2j} - t_k F_{2j} + J_x F_{3j},\\
(\omega + \xi_y)F_{2j} &= \Delta^{*}_{2k}G_{1j} + \Delta^{*}_{4k}G_{2j} - t_k F_{1j} + J_y F_{3j},\\
(\omega + \xi_L)F_{3j} &= \frac{\Delta^{*}_{5k}}{K_k}G_{3j} + (J_x F_{1j} + J_y F_{2j})K_k.
\end{aligned} \tag{11}$$

Here, we have introduced the following notation for normal Green's functions

$$G_{11} = \langle\langle a_{k\uparrow}|a^{\dagger}_{k\uparrow}\rangle\rangle_{\omega}, \quad G_{21} = \langle\langle b_{k\uparrow}|b^{\dagger}_{k\uparrow}\rangle\rangle_{\omega},$$
$$G_{31} = \langle\langle L_{k\uparrow}|a^{\dagger}_{k\uparrow}\rangle\rangle_{\omega}.$$

Functions G_{i2} and G_{i3} ($i = 1, 2, 3$) are defined analogously, the only difference being that operators $b^{\dagger}_{k\uparrow}$ and $L^{\dagger}_{k\uparrow}$ appear, respectively, instead of $a^{\dagger}_{k\uparrow}$. The anomalous Green functions are defined as

$$F_{11} = \langle\langle a^{\dagger}_{-k\downarrow}|a^{\dagger}_{k\downarrow}\rangle\rangle_{\omega}, \quad F_{21} = \langle\langle b^{\dagger}_{-k\downarrow}|b^{\dagger}_{k\uparrow}\rangle\rangle_{\omega},$$
$$F_{31} = \langle\langle L^{\dagger}_{-k\downarrow}|a^{\dagger}_{k\uparrow}\rangle\rangle_{\omega}.$$

For functions F_{i2} and F_{i3} ($i = 1, 2, 3$), we are using the same notation for the second subscript as for the normal functions.

In writing system of equations (11), we have used functions

$$\begin{aligned}
\xi_{x(y)} &= \xi_{k_{x(y)}}, \quad J_{x(y)} = Js_{k,x(y)},\\
\xi_L(k) &= \tilde{\varepsilon}_p - \mu - 2t + 5\tau/2 - J\\
&+ [(\tau - 2t)(-C_1\gamma_{1k} + C_2\gamma_{2k})\\
&+ \tau(-C_1\gamma_{1k} + C_3\gamma_{3k})/2\\
&+ JC_1(1 + 4\gamma_{1k})/4 - IC_1(\gamma_{1k} + 4)]K_k^{-1},
\end{aligned} \tag{12}$$

where $K_k = \langle\{L_{k\uparrow}, L^{\dagger}_{k\uparrow}\}\rangle = 3/4 - C_1\gamma_{1k}$, and γ_{jk} denote invariants of the square lattice:

$$\gamma_{1k} = (\cos k_x + \cos k_y)/2, \quad \gamma_{2k} = \cos\gamma_x \cos k_y,$$
$$\gamma_{3k} = (\cos 2k_x + \cos 2k_y)/2.$$

The superconducting order parameter components are connected with anomalous means by the following relations:

$$\begin{aligned}
\Delta_{1k} &= -\frac{2}{N}\sum_q \left(\frac{U_p}{2} + V_2\cos(k_y - q_y)\right.\\
&\left. + V_2'\cos(k_x - q_x)\right)\langle a_{q\uparrow}a_{-q\downarrow}\rangle,\\
\Delta_{2k} &= -\frac{4V_1}{N}\sum_q \phi_{k-q}\langle a_{q\uparrow}b_{-q\downarrow}\rangle,\\
\Delta_{3k} &= -\frac{4V_1}{N}\sum_q \phi_{k-q}\langle b_{q\uparrow}a_{-q\downarrow}\rangle,\\
\Delta_{4k} &= -\frac{2}{N}\sum_q \left(\frac{U_p}{2} + V_2\cos(k_x - q_x)\right.\\
&\left. + V_2'\cos(k_y - q_y)\right)\langle b_{q\uparrow}b_{-q\downarrow}\rangle,\\
\Delta_{5k} &= \frac{1}{N}\sum_q \{I_{k-q}(\langle L_{q\uparrow}L_{-q\downarrow}\rangle - C_1\langle b_{q\uparrow}u_{-q\downarrow}\rangle)\\
&+ 8IC_1\langle u_{q\uparrow}u_{-q\downarrow}\rangle\} + \frac{J}{N}\sum_q \left\{-2\gamma_{1q}\langle L_{q\uparrow}L_{-q\downarrow}\rangle\right.\\
&\left. + \left(\frac{3}{2} - 4C_1\gamma_{1k}\right)\langle u_{q\uparrow}u_{-q\downarrow}\rangle\right\}\\
&+ \frac{2}{N}\sum_q (\xi(q_x)s_{q,x} + t_q s_{q,y})\langle a_{q\uparrow}L_{-q\downarrow}\rangle\\
&+ \frac{2}{N}\sum_q (\xi(q_y)s_{q,y} + t_q s_{q,x})\langle b_{q\uparrow}L_{-q\downarrow}\rangle\\
&- \frac{U_p}{N}\sum_q \left\{\left(\frac{3}{8} - \frac{C_1}{2}\cos k_x\right)\langle a_{q\uparrow}a_{-q\downarrow}\rangle\right.\\
&\left. + \left(\frac{3}{8} - \frac{C_1}{2}\cos k_y\right)\langle b_{q\uparrow}b_{-q\downarrow}\rangle\right\}\\
&- \frac{V_1}{N}\sum_q \left\{\left(\frac{3}{4} - 2C_1\gamma_{1k} + C_2\gamma_{2k}\right)\psi_q\right.\\
&\left. + C_2\sin k_x \sin k_y \phi_q\right\}(\langle a_{q\uparrow}b_{-q\downarrow}\rangle + \langle b_{q\uparrow}a_{-q\downarrow}\rangle)\\
&- \frac{1}{N}\sum_q \{V_2(C_1\cos k_y - C_2\gamma_{2k})\cos q_y\\
&+ V_2'\left(-\frac{3}{8} + C_1\cos k_x - \frac{C_3}{2}\cos 2k_x\right)\cos q_x\Big\}\langle a_{q\uparrow}a_{-q\downarrow}\rangle\\
&- \frac{1}{N}\sum_q \{V_2(C_1\cos k_x - C_2\gamma_{2k})\cos q_x\\
&+ V_2'\left(-\frac{3}{8} + C_1\cos k_y - \frac{C_3}{2}\cos 2k_y\right)\cos q_y\Big\}\langle b_{q\uparrow}b_{-q\downarrow}\rangle,
\end{aligned} \tag{13}$$

where

$$I_k = 4I\gamma_{1k}, \quad \phi_k = \cos\frac{k_x}{2}\cos\frac{k_y}{2},$$

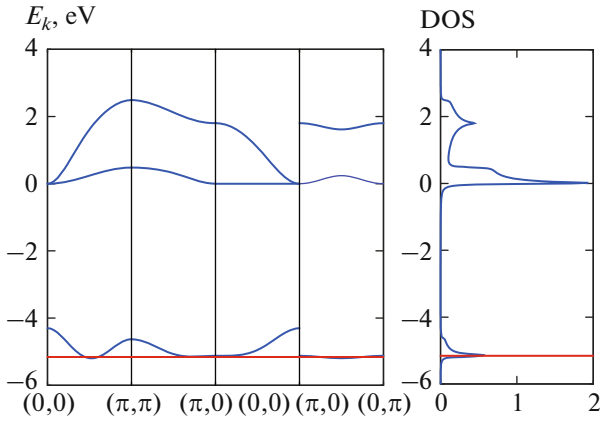

Fig. 2. (Color online) Energy structure and density of states (DOS) in the spin–fermion model in the normal phase, calculated for the following set of parameters (in electronvolts): $t_{pd} = 1.3$, $\Delta_{pd} = 3.6$, $U_d = 10.5$, $V_{pd} = 1.2$, $U_p = V_1 = V_2 = 0$, and $t = 0.12$. The lower branch ϵ_{1k} corresponds to spin-polaron excitations. Red line indicates the position of chemical potential μ.

$$\psi_k = \sin\frac{k_x}{2}\sin\frac{k_y}{2}$$

and the mean is given by

$$\langle u_{q\uparrow}u_{-q\downarrow}\rangle = -s^2_{q,x}\langle a_{q\uparrow}a_{-q\downarrow}\rangle - s^2_{q,y}\langle b_{q\uparrow}b_{-q\downarrow}\rangle - \psi_q(\langle a_{q\uparrow}b_{-q\downarrow}\rangle + \langle b_{q\uparrow}a_{-q\downarrow}\rangle). \quad (14)$$

In deriving system of equations (11), we considered that the subsystem of localized spins at copper ions is in the quantum liquid state. In this case, spin correlation functions $C_j = \langle S_0 S_{r_j}\rangle$ appearing in expressions (12) and (13) satisfy relations

$$C_j = 3\langle S^x_0 S^x_{r_j}\rangle = 3\langle S^y_0 S^y_{r_j}\rangle = 3\langle S^z_0 S^z_{r_j}\rangle, \quad (15)$$

where r_j is the coordinate of the copper ion in the jth coordination sphere. In this case, $\langle S^x_f\rangle = \langle S^y_f\rangle = \langle S^z_f\rangle = 0$. The dependence of correlators C_j on the doping level was determined simultaneously using the spherically symmetric self-consistent approach for a frustrated antiferromagnet [48]. Since we are interested in the low doping regime, the contributions in expressions (12) and (13), which appear as a result of uncoupling of means and are proportional to correlators of the density–density type, are not considered here.

4. NORMAL PHASE OF SPIN POLARONS

Analysis of system of equations (11) for the normal phase shows that the Fermi excitation spectrum in the SFM is determined by the solutions to dispersion equation

$$\det_k(\omega) = (\omega - \xi_k)(\omega - \xi_y)(\omega - \xi_L) - 2J_xJ_yt_kK_k - (\omega - \xi_y)J^2_xK_k - (\omega - \xi_x)J^2_yK_k - (\omega - \xi_L)t^2_k = 0 \quad (16)$$

and consists of three branches, ϵ_{1k}, ϵ_{2k}, and ϵ_{3k} (Fig. 2) [31]. It can be seen from Fig. 2 that lower branch ϵ_{1k} is characterized by a minimum near point $(\pi/2, \pi/2)$ of the Brillouin zone and is considerably spaced from two upper bands ϵ_{2k} and ϵ_{3k}. The lower branch appears due to the strong spin–charge coupling that induces the exchange interaction between holes at spins localized at the nearest copper ions, as well as spin-correlated jumps. For low doping levels x, the dynamics of holes at oxygen ions is determined exclusively by the lower band with dispersion ϵ_{1k}.

Analysis of the modification of density of Fermi states [49], which is induced by the change in the value of hopping integral for holes at oxygen ions, has shown that a decrease in t leads to a shift of the Van Hove singularity of the spin-polaron band shown in Fig. 2 and, as a consequence, to a displacement of the peak on the concentration dependence of the superconducting transition temperature towards lower hole number densities (see Section 5).

Figure 3 shows the modification of the Fermi surface under doping in the case when chemical potential μ lies in lower band ϵ_{1k}. It can be seen that in the range of small values of x corresponding to incompletely doped cuprates, the Fermi surface is strongly anisotropic. Estimation of the effective mass of spin-polaron quasiparticles in the nodal ($\Gamma - M$) direction gives value of $m_{\Gamma - M} = 1.25m_e$, where m_e is the free electron mass. In the antinodal ($X - X$) direction, the effective mass is $m_{X - X} = 9.4m_e$ [50]. At doping level $x \approx 0.16$, the Fermi surface topology changes from the electron to hole type.

5. STABILITY OF d-WAVE PAIRING OF SPIN POLARONS TO COULOMB INTERACTIONS

For analyzing the condition for the emergence of Cooper instability in the linear approximation, the required anomalous Green functions are expressed in terms of parameters Δ^*_{lk} ($l = 1, ..., 5$). Then expressions for anomalous means are derived using the spectral theorem [51], and a closed system of homogeneous integral equations is obtained for the superconducting order parameter components:

$$\Delta^*_{1k} = -\frac{2}{N}\sum_{lq}\left(\frac{U_p}{2} + V_2\cos k_y\cos q_y + V_2'\cos k_x\cos q_x\right)M^{(l)}_{11}(q)\Delta^*_{lq},$$

$$\Delta^*_{2k} = -\frac{4V_1}{N}\sum_{lq}\phi_{k-q}M^{(l)}_{21}(q)\Delta^*_{lq},$$

$$\Delta^*_{3k} = -\frac{4V_1}{N}\sum_{lq}\phi_{k-q}M^{(l)}_{12}(q)\Delta^*_{lq},$$

$$\Delta^*_{4k} = -\frac{2}{N}\sum_{lq}\left(\frac{U_p}{2} + V_2\cos k_x\cos q_x + V_2'\cos k_y\cos q_y\right)M^{(l)}_{22}(q)\Delta^*_{lq}, \quad (17)$$

$$\Delta^*_{5k} = -\frac{1}{N}\sum_{lq}R^{(l)}_0(q)\Delta^*_{lq} + \frac{1}{N}\sum_{lq}I_{k-q}R^{(l)}_{1a}(q)\Delta^*_{lq}$$
$$+\cos k_x\frac{1}{N}\sum_{lq}R^{(l)}_{1b}(q)\Delta^*_{lq} + \cos k_y\frac{1}{N}\sum_{lq}R^{(l)}_{1c}(q)\Delta^*_{lq}$$
$$-\gamma_{2k}\frac{1}{N}\sum_{lq}R^{(l)}_2(q)\Delta^*_{lq} - \sin k_x\sin k_y\frac{1}{N}\sum_{lq}\phi_q R^{(l)}_3(q)\Delta^*_{lq}$$
$$-\cos 2k_x\frac{1}{N}\sum_{lq}R^{(l)}_{4a}(q)\Delta^*_{lq} - \cos 2k_y\frac{1}{N}\sum_{lq}R^{(l)}_{4b}(q)\Delta^*_{lq}.$$

Here, we have introduced functions

$$R^{(l)}_0(q) = \frac{3}{4}V_1\psi_q M^{(l)}_{ab}(q) + 2J\gamma_{1q}M^{(l)}_{33}(q)$$
$$-\left(8IC_1 + \frac{3J}{2}\right)M^{(l)}_{uu}(q) + \frac{3}{8}U_p(M^{(l)}_{11}(q) + M^{(l)}_{22}(q))$$
$$-2(\xi(q_x)s_{q,x} + t_q s_{q,y})M^{(l)}_{31}(q)$$
$$-2(\xi(q_y)s_{q,y} + t_q s_{q,x})M^{(l)}_{32}(q)$$
$$-\frac{3}{8}V_2'\cos q_x M^{(l)}_{11}(q) - \frac{3}{8}V_2'\cos q_y M^{(l)}_{22}(q),$$

$$R^{(l)}_{1b}(q) = C_1(V_1\psi_q M^{(l)}_{ab}(q) - 2JM^{(l)}_{uu}(q) + U_p M^{(l)}_{11}(q)$$
$$-V_2'\cos q_x M^{(l)}_{11}(q) - V_2\cos q_x M^{(l)}_{22}(q)),$$

$$R^{(l)}_{1c}(q) = C_1(V_1\psi_q M^{(l)}_{ab}(q) - 2JM^{(l)}_{uu}(q) + U_p M^{(l)}_{22}(q)$$
$$-V_2\cos q_y M^{(l)}_{11}(q) - V_2'\cos q_y M^{(l)}_{22}(q)),$$

$$R^{(l)}_2(q) = C_2(V_1\psi_q M^{(l)}_{ab}(q) - V_2\cos q_y M^{(l)}_{11}(q)$$
$$-V_2\cos q_x M^{(l)}_{22}(q)),$$

$$R^{(l)}_3(q) = V_1 C_2 M^{(l)}_{ab}(q),$$

$$R^{(l)}_{4a}(q) = -\frac{V_2'}{2}C_3\cos q_x M^{(l)}_{11}(q),$$

$$R^{(l)}_{4b}(q) = -\frac{V_2'}{2}C_3\cos q_y M^{(l)}_{22}(q),$$

$$M^{(l)}_{uu}(q) = -s^2_{qx}M^{(l)}_{11}(q) - s^2_{qy}M^{(l)}_{22}(q) - \psi_q M^{(l)}_{ab}(q),$$

$$M^{(l)}_{ab}(q) = M^{(l)}_{21}(q) + M^{(l)}_{12}(q),$$

$$M^{(l)}_{nm}(q) = \frac{S^{(l)}_{nm}(q, E_{1q}) + S^{(l)}_{nm}(q, -E_{1q})}{4E_{1q}(E^2_{1q} - E^2_{2q})(E^2_{1q} - E^2_{3q})}\tanh\frac{E_{1q}}{2T},$$

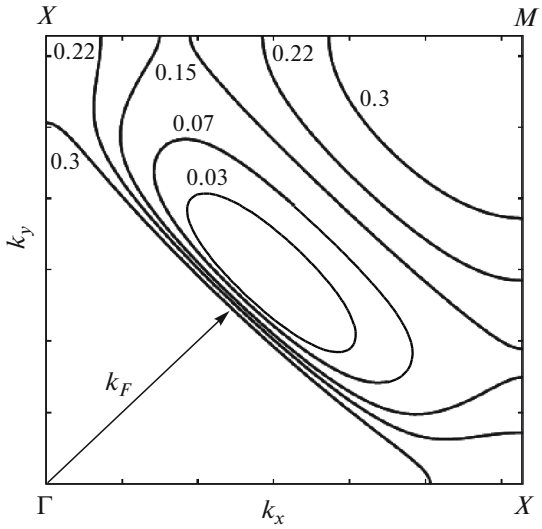

Fig. 3. Fermi surfaces in the first quadrant of the Brillouin zone for five values of the doping level. Doping level x is indicated on the relevant Fermi contour.

and corresponding functions $S^{(l)}_{ij}(k, \omega)$ are given in Appendix. The system of equations (17) is used for determining the superconducting transition temperature with preset types of the order parameter symmetry.

It can be seen from Eqs. (17) that the kernels of the integral equations are split; therefore, we can seek the solution to the system in the form

$$\begin{aligned}
\Delta_{1k} &= B_{11} + B_{12}\cos k_x + B_{13}\cos k_y,\\
\Delta_{2k} &= B_{21}\phi_k + B_{22}\psi_k,\\
\Delta_{3k} &= B_{31}\phi_k + B_{32}\psi_k,\\
\Delta_{4k} &= B_{41} + B_{42}\cos k_x + B_{43}\cos k_y,\\
\Delta_{5k} &= B_{51} + B_{52}\cos k_x + B_{53}\cos k_y\\
&+ B_{54}\cos k_x\cos k_y + B_{55}\sin k_x\sin k_y\\
&+ B_{56}\cos 2k_x + B_{57}\cos 2k_y,
\end{aligned} \quad (18)$$

where seventeen amplitudes B determine the contribution of the corresponding basis functions to the expansion of order parameter components. Substituting these expressions into Eqs. (17) and equating the coefficients of the corresponding trigonometric functions, we obtain a system of seventeen algebraic equations for amplitudes B. The solution of this system together with the equation for chemical potential μ,

$$x = \frac{2}{N}\sum_q\frac{f(\epsilon_{1q})[Q_{3x}(q, \epsilon_{1q}) + Q_{3y}(q, \epsilon_{1q})]}{(\epsilon_{1q} - \epsilon_{2q})(\epsilon_{1q} - \epsilon_{3q})}, \quad (19)$$

make it possible to find the dependence of superconducting transition temperature T_c on doping level x for various types of the order parameter symmetry. In Eq. (19), $f(E) = (e^{E/T} + 1)^{-1}$ denotes the Fermi–Dirac

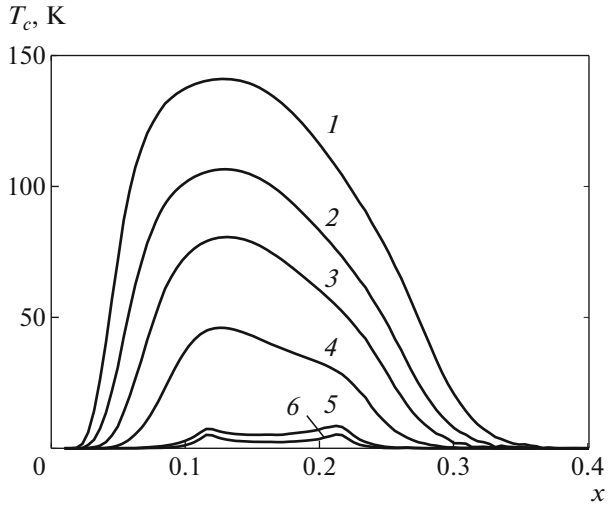

Fig. 4. Dependences of the superconducting transition temperature for the $d_{x^2-y^2}$-wave type of pairing on the doping level, obtained for the following model parameters (in electronvolts): $J = 3.38$, $\tau = 0.10$, $t = 0.12$, and $I = 0.136$ for $U_p = V_2 = 0$ (curve *1*), $U_p = 0$, $V_2 = 0.2$ (curve *2*), $U_p = 3$, $V_2 = 0$ (curve *3*), $U_p = 3$. $V_2 = 0.2$ (curve *4*), $U_p = 0$, $V_2 = 0.8$ (curve *5*), and $U_p = 3$, $V_2 = 0.5$ (curve *6*).

distribution function; functions $Q_{3x}(k, \omega)$ and $Q_{3y}(k, \omega)$ are given in Appendix.

The results of numerical self-consistent solution are shown in Fig. 4. Curve *1* shows the dependence of the superconducting transition temperature of superconducting $d_{x^2-y^2}$-wave pairing on the doping level for $U_p = V_1 = V_2 = 0$. This curve was obtained earlier in [31] and is in good agreement with experimental data as regards the absolute value of T_c as well as the doping interval in which Cooper instability evolves.

An important aspect of the approach developed here is that the inclusion of Coulomb interaction V_1 of fermions located at the nearest oxygen ions does not affect the $T_c(x)$ dependence for the superconducting $d_{x^2-y^2}$-wave pairing: curve *1* in Fig. 4 remains unchanged [32]. The reason for such a behavior can be established after analysis of the solution to system of integral equations (17). In the doping region in which the above type of pairing is realized at $T \lesssim T_c$, the solutions to the algebraic system for amplitudes B show that only four of these amplitudes (B_{52}, B_{53}, B_{22}, and B_{32}) differ from zero and $B_{52} = -B_{53}$, $B_{22} = -B_{32}$, and $|B_{52}|/|B_{22}| \sim 10^3$. This means that the quasi-momentum dependence of the superconducting gap width is mainly determined by fifth order parameter component Δ_{5k} that has form

$$\Delta_{5k}^{(d)} = B_{52}(\cos k_x - \cos k_y). \tag{20}$$

For the superconducting $d_{x^2-y^2}$-wave pairing for $U_p = V_2 = 0$, amplitudes B_{52} and B_{53} in the equation for Δ_{5k} are determined exclusively by exchange constant I and not by parameter V_1 and, hence, the intersite Coulomb repulsion for holes at neighboring oxygen ions does not suppress the Cooper instability in the d-wave channel [32].

In this case, instead of the system of 17 equations, we can obtain and solve a simpler equation for T_c [31, 49, 52], which follows from the fifth equation of system (17) and has form

$$1 = \frac{I}{N}\sum_q (\cos q_x \cos q_y)^2 \times (M_{33}^{(5)}(q, \epsilon_{1q}) - C_1 M_{uu}^{(5)}(q, \epsilon_{1q})). \tag{21}$$

In particular, this equation implies that the mechanism responsible for the emergence of superconducting pairing is the exchange interaction of spin moments of copper ions, which is transformed into effective attraction due to the strong spin–charge coupling. The results of solution of Eq. (21) and the system of seventeen equations for amplitudes B for d-wave pairing obviously coincide for $U_p = V_2 = 0$ and correspond to curve *1* in Fig. 4.

In contrast to the intersite interaction of holes at two nearest oxygen ions, the inclusion of Coulomb interaction U_p for two holes at the same oxygen ion leads to suppression of the d-wave superconducting phase. However, comparison of curve *3* ($U_p = 3$ eV and $V_2 = 0$) and curve *1* ($U_p = V_2 = 0$) in Fig. 4 shows that this suppression is insignificant for realization of HTSC because the superconducting transition temperature in the region of optimal doping level $x \simeq 0.6$ remains high.

Let us consider the effect of Coulomb repulsions V_2 of holes located at the next-to-nearest oxygen ions in the CuO_2 plane on superconducting pairing. Curve *2* in Fig. 4 corresponds to the $T_c(x)$ dependence obtained for $U_p = 0$, $V_2 = 0.2$ eV, while curve *5* corresponds to $T_c(x)$ for $U_p = 0$ and $V_2 = 0.8$ eV. It can be seen that the inclusion of V_2, in contract to the inclusion of V_1, leads to suppression of the superconducting $d_{x^2-y^2}$-wave pairing. This suppression becomes stronger if $U_p \neq 0$ (curves *3*, *4*, and *6*). However, even when the aforementioned Coulomb interactions are taken into account simultaneously, the $d_{x^2-y^2}$-wave pairing is preserved and can be suppressed only for unrealistically high values of $V_2 > 0.5$ eV [33, 34].

Figure 5 shows a modification of the gap in the elementary excitation spectrum for spin-polaron quasiparticles on the Fermi contour in the superconducting phase upon a change in Coulomb interactions U_p and V_2, which was calculated in [53]. It can be seen from the figure that the quasi-momentum dependence of the gap width in the first Brillouin zone is character-

ized by the $d_{x^2-y^2}$-wave type of order parameter symmetry. Since Coulomb interaction V_1 of holes at neighboring oxygen ions does not affect the superconducting d-wave pairing, the behavior of the superconducting gap is determined only by three order parameter components Δ_{1k}, Δ_{4k}, and Δ_{5k} from system (13). The self-consistent solution of the system of three equations for these components together with the equation for chemical potential (now without using the approximation linear in Δ_{jk} in determining the required anomalous Green's functions) leads to the $\Delta(k)$ dependences shown in Fig. 5.

An important aspect concerning the realization of the s-wave pairing in an ensemble of spin polarons was considered for simplicity disregarding the long-range Coulomb interaction ($V_2 = 0$). In this case, system of integral equations (17) implies that the solution corresponding to the superconducting s-wave phase must have form

$$\Delta_{1k}^{(s)} = \Delta_{4k}^{(s)} = B_{11},$$
$$\Delta_{2k}^{(s)} = \Delta_{3k}^{(s)} = 0, \qquad (22)$$
$$\Delta_{5k}^{(s)} = B_{51} + 2B_{52}\gamma_{1k} + B_{54}\gamma_{2k}.$$

Calculations show that for all realistic model parameters, the system has no nontrivial solution corresponding to the s-wave pairing [35]. Consequently, in the spin–fermion model that correctly takes into consideration the strong coupling between holes at oxygen ions with the spin moments of copper ions, the superconducting phase with the s-wave order parameter symmetry is not realized.

6. LONDONS PENETRATION DEPTH

The spin-polaron approach that proved to be successful in the description of equilibrium properties of the hole-doped cuprates in the normal as well as in the superconducting phase can also be used for analyzing the response of the system to electromagnetic perturbation. This is confirmed by the result obtained in [54], where the temperature dependence of the magnetic field penetration depth in a superconductor in which spin-polaron quasiparticles play the role of charge carriers was investigated at different doping levels.

In the local approximation, the relation between superconducting current density $\mathbf{j}$ and vector potential $\mathbf{A}$ of the magnetic field is described by the Londons equation

$$\mathbf{j} = -\frac{c}{4\pi\lambda^2}\mathbf{A}, \qquad (23)$$

where λ is the magnetic field penetration depth in the superconductor and c is the velocity of light. For calculating superconducting current density $\mathbf{j}$, we supplement SFM Hamiltonian (2) written in the Wannier representation with the magnetic field written in the Peierls approximation. This substitution leads to renormalization of all hopping integrals by the phase factor

$$\exp\left\{\frac{ie}{c\hbar}R_{mn}^{x}A_{q=0}^{x}\right\}, \qquad (24)$$

where $R_{mm} = R_m - R_n$ is the difference between the radius vectors for sites with subscripts m and n, e is the electron charge, and $A_{q=0}^{x}$ is the Fourier component of the vector potential, which is considered in the long-wave approximation (see, for example, [40]). For simplicity, we choose vector potential $\mathbf{A}$ in the direction of the x axis.

The standard procedure for calculating the paramagnetic and diamagnetic parts of the current involves the separation in the Hamiltonian of linear and quadratic corrections from the value of vector potential $A_{q=0}^{x}$ and subsequent variation of these corrections in $A_{q=0}^{x}$ [40, 55–57]. Departing from the given procedure, we reject the expansion of phase factors (24) into a power series in $A_{q=0}^{x}$ and leave these factors in their initial form. In this case, after passing to the quasi-momentum representation, the only change due to inclusion of magnetic field in formulas (3) and (6) for operators $\hat{H}_h$ and $\hat{J}$ is the formation of additional phase α_x in the argument of trigonometric function $s_{k,x}$ [54]:

$$s_{k,x} \to s_{k,x} = \sin(k_x/2 - \alpha_x), \qquad (25)$$

where

$$\alpha_x = \frac{eg_x}{2c\hbar}A_{q=0}^{x}, \qquad (26)$$

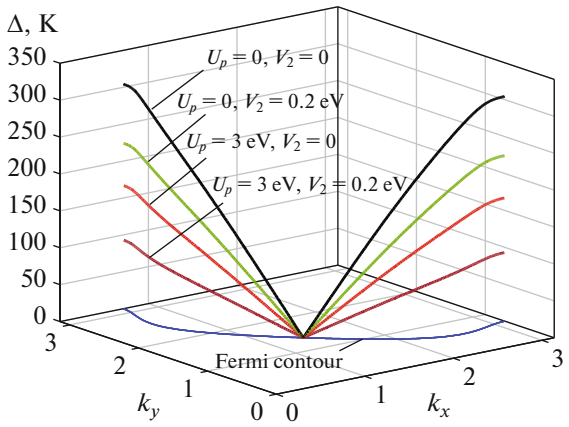

Fig. 5. (Color online) Quasi-momentum dependences of the superconducting gap width on the Fermi contour for $x = 0.125$, $I = 0.136$ eV, $T = 0$, and different values of the Coulomb interactions.

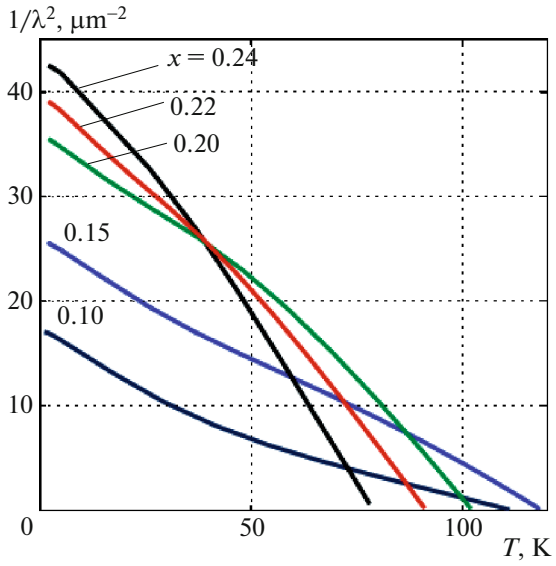

Fig. 6. (Color online) Temperature dependences of the reciprocal square of the Londons penetration depth, which were calculated for different doping levels x for the following set of model parameters (in electronvolts): $\tau = 0.225$, $J = 2.86$, $I = 0.118$, $t = 0.12$, and $U_p = V_2 = V_2' = 0$.

and g_x is the lattice constant along the x axis. Function $s_{k,y}$ remains unchanged because $A^y_{q=0} = 0$ in the given case.

The variations of expressions for operators $\hat{H}_h$ and $\hat{J}$ in the vector potential lead to the following expression for the superconducting current density:

$$j_x = \frac{eg_x}{\hbar}\sum_{k\alpha}\cos\left(\frac{k_x}{2} - \alpha_x\right)[2\tau s_{k,x}\langle a^\dagger_{k\alpha}a_{k\alpha}\rangle + (2\tau - 4t)s_{k,y}\langle a^\dagger_{k\alpha}b_{k\alpha}\rangle + J\langle a^\dagger_{k\alpha}L_{k\alpha}\rangle]. \quad (27)$$

The dependence of j_x on the vector potential in the range of small $A^x_{q=0}$ must be linear, and the factor determining this linear dependence can be directly expressed in terms of λ^{-2} in accordance with the Londons equation. This factor was calculated numerically [54], and the results of calculation of the temperature dependence of the magnetic penetration depth in a spin-polaron ensemble are shown in Fig. 6 for different doping levels.

In spite of the fact that model parameters were not determined from fitting, but were chosen to be equal to those used in previous publications (see Section 2), the curves shown in Fig. 6 demonstrate satisfactory agreement with experimental data [58–66]. At a low temperature, all curves exhibit the linear behavior down to the lowest of considered temperature $T = 2$ K. Such a behavior indicates, according to the results obtained in [59], the d-wave symmetry type of the superconducting order parameter. For values of x corresponding to overdoped samples of cuprate superconductors ($x \gtrsim 0.16$), the $\lambda^{-2}(T)$ curves are convex, which agrees with the most of experimental data [60, 61, 65].

Apart from dependences $\lambda^{-2}(T)$, an important result obtained in [54] was the derivation of the analytic expression for spin-polaron spectrum E_k in the superconducting phase with account for the vector potential. Considering that the charge carrier concentration is low and the energy gap between the lower spin-polaron band and the energy level of holes on p-orbitals of oxygen is large (on the order of J) (see Fig. 2), the expression for E_k could be written in "classical" form

$$E_k = \delta\epsilon_{1k} + \sqrt{\epsilon^2_{1k} + \Delta^2_k}, \quad (28)$$

where $\delta\epsilon_{1k}$ is the correction to the polaron spectrum ϵ_{1k} which is linear in α_x, and gap function Δ^2_k was expressed only in terms of order parameter component Δ_{5k},

$$\Delta^2_k = |\Delta_{5k}|^2/K^2_k,$$

because the contributions from Coulomb interactions $\hat{U}_p$ and $\hat{V}_{pp}$ were disregarded in [54].

Since the inclusion of this interactions leads to the emergence of additional order parameter components in system of equations (11), it is necessary to generalize the expressions for Δ^2_k. Calculations show that when the Coulomb interaction is taken into account, each order parameter component Δ_{jk} ($j = 1, ..., 5$) makes its additive contribution to the gap function:

$$\Delta^2_k = |\Delta_{1k}|^2 + |\Delta_{2k}|^2 + |\Delta_{3k}|^2 + |\Delta_{4k}|^2 + \frac{|\Delta_{5k}|^2}{K^2_k}. \quad (29)$$

Concluding this section, we note that in spite of the three-band energy structure of the system, Fermi excitation spectrum E_k for spin polarons in the superconducting phase can be expressed only in terms of spectrum ϵ_{1k} of the lower band in the normal phase. For small values of α_x, the Bogoliubov quasiparticle spectrum is renormalized in the same additive way as in the conventional theory of the Londons penetration depth [55, 57]. At the same time, the special quasi-momentum dependence of spectrum ϵ_{1k} of the normal phase (and, hence, its field-induced corrections $\delta\epsilon_{1k}$) substantially differs from the simplest case of quadratic dispersion and is determined by the structure of the CuO_2 plane and the strong spin–fermion interaction.

7. CONCLUSIONS

It has been shown that low-temperature properties of cuprate superconductors described using the SFM model are determined by spin-polaron quasiparticles.

Upon cooling, an ensemble of these quasiparticles demonstrates Cooper instability with the $d_{x^2-y^2}$-wave type of the order parameter symmetry. The role of the superconducting pairing mechanism is played by the exchange interaction between spins localized at copper ions, which is transformed into effective attraction between spin polarons as a result of the strong spin–charge coupling.

It has been demonstrated that neutralization of the negative effect of intersite Coulomb interaction of holes on the superconducting $d_{x^2-y^2}$-wave type of pairing occurs because of two factors. One factor is associated with analysis of the actual crystallographic structure of the copper–oxygen plane, in accordance with which the Coulomb repulsion of fermions in the oxygen sublattice is determined by the Fourier transform of the intersite Coulomb interaction,

$$V_q = 4V_1 \cos(q_x/2)\cos(q_y/2).$$

The other factor is associated with electron correlations leading to the emerging of a strong spin–charge coupling. In this case, the Coulomb repulsion between bare holes with Fourier transform V_q is renormalized into the interaction between spin polarons so that the quasi-momentum dependence of this effective interaction corresponds to the structure of the copper ion sublattice. Therefore, the situation arises in which the effective repulsion between spin-polaron quasiparticles is omitted from the equation for the superconducting order parameter with the $d_{x^2-y^2}$-wave symmetry type.

It is appropriate to note in this connection that an analogous problem of neutralization of the effect of Coulomb repulsion of fermions on the evolution of Cooper instability also existed in the theory of classical superconductors. This problem could be solved after it had been proven [67, 68] that the electron–phonon interaction in a certain region of the momentum space initiates effective attraction between fermions, which can compensate for the initial repulsion.

It should also be noted that different contributions of the Coulomb interaction to the realization of superconducting phases with different types of the order parameter symmetry are also manifested in the Kohn–Luttinger theory of superconductivity [69]. It was established in [70, 71] that intersite Coulomb interactions in lattice models usually contribute to only certain pairing channels and do not affect other channels. At the same time, polarization contributions have components in all channels, and more than one component facilitates attraction as a rule. It turns out that intersite interactions in such a situation either do not affect the main components of the effective interaction leading to pairing, or suppress the main component without influencing on secondary ones [70, 71]. In our case, the peculiarities of the crystallographic structure of the CuO_2 plane play a decisive role when both types of oxygen orbitals spatially separated from the spins of copper ions as well as the existence of strong spin–charge coupling are taken into account.

In this study, it is shown that Hubbard repulsion U_p as well as Coulomb interactions V_2 of holes at the next-to-nearest oxygen ions affect the formation of the superconducting phase with the *d*-wave type of the order parameter symmetry and lead to a decrease in the superconducting transition temperature; however, this temperature remains in the range of experimentally observed values. The formation of the superconducting gap occurs in this case under the influence of three order parameter components.

The solution of the system of self-consistent integral equations for the superconducting state shows that only the phase with the $d_{x^2-y^2}$-wave type of the order parameter symmetry is realized in the spin-fermion model, while the solutions for the superconducting *s*-wave pairing are absent for all admissible doping levels.

The calculation of the temperature and concentration dependences of the Londons penetration depth in the semiconductor has been used as an example for demonstrating the possibility of application of the spin–polaron approach to analysis of the system response to an external electromagnetic perturbation. The obtained dependences are in good agreement with experimental data on cuprate superconductors.

Concluding the section, let us briefly outline important trends in further application of the spin-polaron conception. One of such trends is the construction of the effective single-orbital model [72] operating in the truncated Hilbert space and including correctly both the peculiarities in the crystallographic structure of the CuO_2 plane and the strong spin–fermion coupling that ensures the formation of spin-polaron quasiparticles. The construction of such a model is important, because analysis of low-temperature properties of cuprate superconductors in the framework of the SFM and even using its simplified version known as the φ–*d* model [49, 52] is still cumbersome. In particular, a transition to such an effective model will make it possible to reduce the rank of the system of self-consistent integral equations for the superconducting phase.

Another trend in further application of the spin-polaron conception is analysis of the conditions for the emergence of spectral intensity modulation on the Fermi contour and of the manifestations of the pseudogap state in an ensemble of spin-polaron quasiparticles [73].

Finally, analysis of kinetic, thermodynamic, and galvanomagnetic characteristics of cuprate superconductors in which spin-polaron quasiparticles play the role of charge carriers [74–77] considering the actual crystallographic peculiarities of the CuO_2 plane appears as quite topical.

APPENDIX

Functions $S_{ij}^{(l)}(k, \omega)$ appearing in the expressions for anomalous Green functions $F_{ij}(k, \omega)$ have the form

$$
\begin{gathered}
S_{11}^{(1)}(k,\omega) = Q_{3y}(k,-\omega)Q_{3y}(k,\omega),\\
S_{11}^{(2)}(k,\omega) = S_{21}^{(1)}(k,\omega) = Q_{3}(k,-\omega)Q_{3y}(k,\omega),\\
S_{11}^{(3)}(k,\omega) = S_{12}^{(1)}(k,\omega) = S_{11}^{(2)}(k,-\omega),\\
S_{11}^{(4)}(k,\omega) = S_{12}^{(2)}(k,\omega)\\
= S_{21}^{(3)}(k,\omega) = S_{22}^{(1)}(k,\omega) = Q_{3}(k,-\omega)Q_{3}(k,\omega),\\
S_{11}^{(5)}(k,\omega) = -Q_{y}(k,-\omega)Q_{y}(k,\omega),\\
\\
S_{12}^{(3)}(k,\omega) = Q_{3y}(k,-\omega)Q_{3x}(k,\omega),\\
S_{21}^{(2)}(k,\omega) = S_{12}^{(3)}(k,-\omega),\\
S_{12}^{(4)}(k,\omega) = S_{22}^{(3)}(k,\omega) = Q_{3}(k,-\omega)Q_{3x}(k,\omega),\\
S_{21}^{(4)}(k,\omega) = S_{22}^{(2)}(k,\omega) = S_{12}^{(4)}(k,-\omega),\\
\\
S_{12}^{(5)}(k,\omega) = -Q_{y}(k,-\omega)Q_{x}(k,\omega),\\
S_{21}^{(5)}(k,\omega) = S_{12}^{(5)}(k,-\omega),\\
S_{22}^{(4)}(k,\omega) = Q_{3x}(k,-\omega)Q_{3x}(k,\omega),\\
S_{22}^{(5)}(k,\omega) = -Q_{x}(k,-\omega)Q_{x}(k,\omega),\\
\\
S_{31}^{(1)}(k,\omega) = -K_{k}Q_{y}(k,-\omega)Q_{3y}(k,\omega),\\
S_{31}^{(2)}(k,\omega) = -K_{k}Q_{x}(k,-\omega)Q_{3y}(k,\omega),\\
S_{31}^{(3)}(k,\omega) = S_{32}^{(1)}(k,\omega) = -K_{k}Q_{y}(k,-\omega)Q_{3}(k,\omega),\\
S_{31}^{(4)}(k,\omega) = S_{32}^{(2)}(k,\omega) = -K_{k}Q_{x}(k,-\omega)Q_{3}(k,\omega),\\
\\
S_{31}^{(5)}(k,\omega) = Q_{xy}(k,-\omega)Q_{y}(k,\omega),\\
S_{32}^{(3)}(k,\omega) = -K_{k}Q_{y}(k,-\omega)Q_{3x}(k,\omega),\\
S_{32}^{(4)}(k,\omega) = -K_{k}Q_{x}(k,-\omega)Q_{3x}(k,\omega),\\
S_{32}^{(5)}(k,\omega) = Q_{xy}(k,-\omega)Q_{3x}(k,\omega),\\
\\
S_{33}^{(1)}(k,\omega) = -K_{k}^{2}S_{11}^{(5)}(k,\omega),\\
S_{33}^{(2)}(k,\omega) = K_{k}^{2}S_{12}^{(5)}(k,-\omega),\\
S_{33}^{(3)}(k,\omega) = S_{33}^{(2)}(k,-\omega),\\
S_{33}^{(4)}(k,\omega) = K_{k}^{2}S_{22}^{(5)}(k,\omega),\\
S_{33}^{(5)}(k,\omega) = Q_{xy}(k,-\omega)Q_{xy}(k,\omega).
\end{gathered}
\tag{30}
$$

These expression include functions

$$
\begin{gathered}
Q_{x(y)}(k,\omega) = (\omega - \xi_{x(y)})J_{y(x)} + t_{k}J_{x(y)},\\
\\
Q_{3}(k,\omega) = (\omega - \xi_{L})t_{k} + J_{x}J_{y}K_{k},\\
Q_{3x(3y)}(k,\omega) = (\omega - \xi_{L})(\omega - \xi_{x(y)}) - J_{x(y)}^{2}K_{k},\\
\\
Q_{xy}(k,\omega) = (\omega - \xi_{x})(\omega - \xi_{y}) - t_{k}^{2}.
\end{gathered}
\tag{31}
$$

ACKNOWLEDGMENTS

The work was prepared based on the results of XXXVIII Conference on low-temperature physics (NT-38).

FUNDING

This study was supported by the program no. 12 "Fundamental problems in high-temperature superconductivity" of the Presidium of the Russian Academy of Sciences, Russian Foundation for Basic Research (project no. 18-02-00837), the administration of the Krasnoyarsk Krai, Krasnoyarsk Krai Foundation for Supporting the Scientific and Technical Activity under project nos. 18-42-243002 (Manifestations of spin-nematic correlations in spectral characteristics of the electronic structure and their influence on the properties of cuprate superconductors in applications), 18-42-243018 (Contact phenomena and magnetic disorder in the problem of formation and detection of topologically protected edge states in semiconducting nanostructures), and 18-42-240014 (Single-orbital effective model of an ensemble of spin-polaron quasiparticles in the problem of description of the intermediate state and pseudogap behavior of cuprate superconductors), as well as the Council for grants from the President of the Russian Federation (project nos. MK-37.2019.2 and MK-3722.2018.2). The work of A.F.B was supported by the Russian Foundation for Basic Research (project no. 19-02-00509).

REFERENCE

1. V. J. Emery, Phys. Rev. Lett. **58**, 2794 (1987).
2. C. M. Varma, S. Schmitt-Rink, and E. Abrahams, Solid State Commun. **62**, 681 (1987).
3. Yu. B. Gaididei and V. M. Loktev, Phys. Status Solidi B **147**, 307 (1988).
4. J. C. Hubbard, Proc. R. Soc. London, Ser. A **285**, 542 (1965).
5. A. F. Barabanov, L. A. Maksimov, and G. V. Uimin, JETP Lett. **47**, 622 (1988); Sov. Phys. JETP **69**, 371 (1989).
6. P. Prelovšek, Phys. Lett. A **126**, 287 (1988).
7. J. Zaanen and A. M. Oleś, Phys. Rev. B **37**, 9423 (1988).
8. E. B. Stechel and D. R. Jennison, Phys. Rev. B **38**, 4632 (1988).
9. V. J. Emery and G. Reiter, Phys. Rev. B **38**, 4547 (1988).
10. H. Matsukawa and H. Fukuyama, J. Phys. Soc. Jpn. **58**, 2845 (1989).
11. K. M. Shen, F. Ronning, D. H. Lu, F. Baumberger, N. J. C. Ingle, W. S. Lee, W. Meevasana, Y. Kohsaka, M. Azuma, M. Takano, H. Takagi, and Z.-X. Shen, Science (Washington, DC, U. S.) **307**, 901 (2005).
12. M. Vojta, Adv. Phys. **58**, 699 (2009).

13. B. Keimer, S. A. Kivelson, M. R. Norman, S. Uchida, and J. Zaanen, Nature (London, U.K.) **518**, 179 (2015).
14. N. M. Plakida, Phys. C (Amsterdam, Neth.) 531, 39 (2016).
15. N. E. Hussey, Adv. Phys. **51**, 1685 (2002).
16. A. F. Barabanov, V. M. Berezovskii, E. Zhasinas, and L. A. Maksimov, J. Exp. Theor. Phys. **83**, 819 (1996).
17. A. F. Barabanov, R. O. Kuzian, and L. A. Maksimov, Phys. Rev. B **55**, 4015 (1997).
18. B. Lau, M. Berciu, and G. A. Sawatzky, Phys. Rev. Lett. **106**, 036401 (2011).
19. A. F. Barabanov, L. A. Maksimov, and A. V. Mikheyenkov, AIP Conf. Proc. **527**, 1 (2000).
20. A. F. Barabanov, A. A. Kovalev, O. V. Urazaev, A. M. Belemuk, and R. Khain, J. Exp. Theor. Phys. **92**, 677 (2001).
21. A. F. Barabanov, A. V. Mikheenkov, and A. M. Belemuk, JETP Lett. **75**, 107 (2002).
22. L. A. Maksimov, A. F. Barabanov, and R. O. Kuzian, Phys. Lett. A **232**, 286 (1997).
23. L. A. Maksimov, R. Hayn, and A. F. Barabanov, Phys. Lett. A **238**, 288 (1998).
24. A. F. Barabanov, A. A. Kovalev, O. V. Urazaev, and A. M. Belemouk, Phys. Lett. A **265**, 221 (2000).
25. A. P. Kampf and J. R. Schrieffer, Phys. Rev. B **42**, 7967 (1990).
26. D. M. Dzebisashvili, V. V. Val'kov, and A. F. Barabanov, JETP Lett. **98**, 528 (2013).
27. T. Yoshida, X. J. Zhou, D. H. Lu, S. Komiya, Y. Ando, H. Eisaki, T. Kakeshita, S. Uchida, Z. Hussain, and Z.-X. Shen, J. Phys.: Condens. Matter **19**, 125209 (2007).
28. A. F. Barabanov, L. A. Maksimov, and A. V. Mikheenkov, JETP Lett. **74**, 328 (2001).
29. V. V. Val'kov, M. M. Korovushkin, and A. F. Barabanov, JETP Lett. **88**, 370 (2008).
30. V. V. Val'kov, T. A. Val'kova, D. M. Dzebisashvili, and S. G. Ovchinnikov, JETP Lett. **75**, 378 (2002).
31. V. V. Val'kov, D. M. Dzebisashvili, and A. F. Barabanov, Phys. Lett. A **379**, 421 (2015).
32. V. V. Val'kov, D. M. Dzebisashvili, M. M. Korovushkin, and A. F. Barabanov, JETP Lett. **103**, 385 (2016).
33. V. V. Val'kov, D. M. Dzebisashvili, M. M. Korovushkin, and A. F. Barabanov, J. Magn. Magn. Mater. **440**, 123 (2017).
34. V. V. Val'kov, D. M. Dzebisashvili, M. M. Korovushkin, and A. F. Barabanov, J. Low Temp. Phys. **191**, 408 (2018).
35. V. V. Val'kov, D. M. Dzebisashvili, M. M. Korovushkin, and A. F. Barabanov, J. Exp. Theor. Phys. **125**, 810 (2017).
36. S. Misawa, Phys. Rev. B **51**, 11791 (1995).
37. R. J. Radtke, V. N. Kostur, and K. Levin, Phys. Rev. B **53**, R522 (1996).
38. D. E. Sheehy, T. P. Davis, and M. Franz, Phys. Rev. B **70**, 054510 (2004).
39. J. P. Carbotte, K. A. G. Fisher, J. P. F. LeBlanc, and A. J. Nicol, Phys. Rev. B **81**, 014522 (2010).
40. M. V. Eremin, I. A. Larionov, and I. E. Lyubin, J. Phys.: Condens. Matter **22**, 185704 (2010).
41. N. F. Mott, *Metal-Insulator Transitions* (Nauka, Moscow, 1979; Taylor Francis, London, 1974).
42. M. Ogata and H. Fukuyama, Rep. Progr. Phys. **71**, 036501 (2008).
43. M. S. Hybertsen, M. Schluter, and N. E. Christensen, Phys. Rev. B **39**, 9028 (1989).
44. M. H. Fischer and E.-A. Kim, Phys. Rev. B **84**, 144502 (2011).
45. R. Zwanzig, Phys. Rev. **124**, 983 (1961).
46. H. Mori, Progr. Theor. Phys. **33**, 423 (1965).
47. L. M. Roth, Phys. Rev. Lett. **20**, 1431 (1968).
48. A. F. Barabanov, A. V. Mikheenkov, and A. V. Shvartsberg, Theor. Math. Phys. **168**, 1192 (2011).
49. V. V. Val'kov, D. M. Dzebisashvili, and A. F. Barabanov, J. Supercond. Nov. Magn. **29**, 1049 (2016).
50. V. V. Val'kov, D. M. Dzebisashvili, and A. F. Barabanov, JETP Lett. **104**, 730 (2016).
51. D. N. Zubarev, Sov. Phys. Usp. **3**, 320 (1960).
52. V. V. Val'kov, D. M. Dzebisashvili, and A. F. Barabanov, J. Low Temp. Phys. **181**, 134 (2015).
53. V. V. Val'kov, M. M. Korovushkin, and A. F. Barabanov, J. Low Temp. Phys. (2018, in press). https://doi.org/10.1007/s10909-018-02120-3
54. D. M. Dzebisashvili and K. K. Komarov, Eur. Phys. J. B **91**, 278 (2018).
55. J. R. Schrieffer, *Theory of Superconductivity* (Perseus Books, MA, 1999).
56. M. V. Sadovskii, *Diagrammatics. Lectures on Selected Problems in Condensed Matter Theory* (RKhD, Izhevsk, 2010) [in Russian].
57. M. Tinkham, *Introduction to Superconductivity* (Dover, New York, 2004; Atomizdat, Moscow, 1980).
58. I. Bozovic, X. He, J. Wu, and A. T. Bollinger, Nature (London, U.K.) **536**, 309 (2016).
59. W. N. Hardy, D. A. Bonn, D. C. Morgan, R. Liang, and K. Zhang, Phys. Rev. Lett. **70**, 3999 (1993).
60. J. E. Sonier, J. H. Brewer, R. F. Kiefl, G. D. Morris, R. I. Miller, D. A. Bonn, J. Chakhalian, R. H. Heffner, W. N. Hardy, and R. Liang, Phys. Rev. Lett. **83**, 4156 (1999).
61. C. Panagopoulos, B. D. Rainford, J. R. Cooper, W. Lo, J. L. Tallon, J. W. Loram, J. Betouras, Y. S. Wang, and C. W. Chu, Phys. Rev. B **60**, 14617 (1999).
62. R. Khasanov, A. Shengelaya, A. Maisuradze, F. La Mattina, A. Bussmann-Holder, H. Keller, and K. A. Müller, Phys. Rev. Lett. **98**, 057007 (2007).
63. R. Khasanov, S. Strassle, D. di Castro, T. Masui, S. Miyasaka, S. Tajima, A. Bussmann-Holder, and H. Keller, Phys. Rev. Lett. **99**, 237601 (2007).
64. W. Anukool, S. Barakat, C. Panagopoulos, and J. R. Cooper, Phys. Rev. B **80**, 024516 (2009).
65. T. R. Lemberger, I. Hetel, A. Tsukada, and M. Naito, Phys. Rev. B **82**, 214513 (2010).
66. B. M. Wojek, S. Weyeneth, S. Bosma, E. Pomjakushina, and R. Puzniak, Phys. Rev. B **84**, 144521 (2011).
67. H. Fröhlich, Phys. Rev. **79**, 845 (1950).

68. V. V. Tolmachev, Sov. Phys. Dokl. **6**, 800 (1961).
69. M. Yu. Kagan, V. A. Mitskan, and M. M. Korovushkin, Phys. Usp. **58**, 733 (2015).
70. S. Raghu, E. Berg, A. V. Chubukov, and S. A. Kivelson, Phys. Rev. B **85**, 024516 (2012).
71. M. Yu. Kagan, V. V. Val'kov, V. A. Mitskan, and M. M. Korovushkin, JETP Lett. **97**, 226 (2013); J. Exp. Theor. Phys. **117**, 728 (2013).
72. V. V. Val'kov, V. A. Mitskan, D. M. Dzebisashvili, and A. F. Barabanov, J. Low Temp. Phys. **44**, 130 (2018).
73. A. F. Barabanov and A. M. Belemuk, JETP Lett. **87**, 628 (2008).
74. A. M. Belemuk, A. F. Barabanov, and L. A. Maksimov, JETP Lett. **79**, 160 (2004); J. Exp. Theor. Phys. **102**, 431 (2006); JETP Lett. **86**, 321 (2006).
75. A. M. Belemuk and A. F. Barabanov, JETP Lett. **82**, 731 (2005).
76. I. A. Larionov and A. F. Barabanov, JETP Lett. **100**, 712 (2014).
77. A. F. Barabanov, Yu. M. Kagan, L. A. Maksimov, A. V. Mikheyenkov, and T. V. Khabarova, Phys. Usp. **58**, 446 (2015).

Translated by N. Wadhwa